Biochemistry and Biophysics Reports 2 (2015) 160–165

Contents lists available at ScienceDirect

Biochemistry and Biophysics Reports

journal homepage: www.elsevier.com/locate/bbrep

The L33F darunavir resistance mutation acts as a molecular anchor reducing the flexibility of the HIV-1 protease 30s and 80s loops

Benjamin D. Kuiper [a,1], Bradley J. Keusch [a,1], Tamaria G. Dewdney [a], Poorvi Chordia [a,b], Kyla Ross [a], Joseph S. Brunzelle [d], Iulia A. Kovari [a], Rodger MacArthur [b], Hossein Salimnia [c], Ladislau C. Kovari [a,*]

[a] Department of Biochemistry and Molecular Biology, Wayne State University School of Medicine, Detroit, MI, USA
[b] Department of Infectious Diseases, Wayne State University School of Medicine, Detroit, MI, USA
[c] Department of Pathology, Wayne State University School of Medicine, Detroit, MI, USA
[d] Life Sciences Collaborative Access Team and Department of Molecular Pharmacology and Biological Chemistry, Northwestern University, Feinberg School of Medicine, Chicago, IL, USA

ARTICLE INFO

Article history:
Received 26 March 2015
Received in revised form
9 June 2015
Accepted 10 June 2015
Available online 12 June 2015

Keywords:
L33F
Molecular Anchor
Drug resistance
darunavir
HIV-1 protease

ABSTRACT

HIV-1 protease (PR) is a 99 amino acid protein responsible for proteolytic processing of the viral polyprotein – an essential step in the HIV-1 life cycle. Drug resistance mutations in PR that are selected during antiretroviral therapy lead to reduced efficacy of protease inhibitors (PI) including darunavir (DRV). To identify the structural mechanisms associated with the DRV resistance mutation L33F, we performed X-ray crystallographic studies with a multi-drug resistant HIV-1 protease isolate that contains the L33F mutation (MDR769 L33F). In contrast to other PR L33F DRV complexes, the structure of MDR769 L33F complexed with DRV reported here displays the protease flaps in an open conformation. The L33F mutation increases non-covalent interactions in the hydrophobic pocket of the PR compared to the wild-type (WT) structure. As a result, L33F appears to act as a molecular anchor, reducing the flexibility of the 30s loop (residues 29–35) and the 80s loop (residues 79–84). Molecular anchoring of the 30s and 80s loops leaves an open S1/S1′ subsite and distorts the conserved hydrogen-bonding network of DRV. These findings are consistent with previous reports despite structural differences with regards to flap conformation.

1. Introduction

The current standard of care for HIV, HAART, often employs a protease inhibitor (PI) containing regimen [1] but mutations in HIV-1 protease (PR) that develop in treatment-experienced patients decrease the efficacy of all current PIs including DRV [1, 2, 3]. Thus, further analysis of key HIV-1 protease resistance mutations is needed to develop more potent antivirals to combat drug resistance.

Clinical isolates previously obtained from the Wayne State University Infectious Disease Clinic in Detroit, MI contain major drug resistance mutations L33F, I47V, I50V, I54M, L76V, V82I/F, and I84F as well as nonpolymorphicaccessory mutations L10V/G, V11I, I13V, K20T/R, L33I/M, K43T, F53L, A71L, T74P, and L89V. These mutations confer resistance to all FDA approved PIs (http://hivdb.stanford.edu/) [4]. Molecular dynamics simulations with these isolates showed altered PR flap dynamics [5].

To further investigate the role of the L33F mutation, we created a recombinant MDR769 L33F PR and performed X-ray crystallographic studies. L33F was initially identified as an accessory mutation to I54L/M, V32I+I47V, and I84V/I but is now recognized as a non-polymorphic major drug resistance mutation [4,6]. L33F is selected for in patients on a ritonavir pharmacokinetic boosted darunavir (DRV/r) regimen [3], is associated with DRV/r resistance [7], has greatly increased in prevalence since the year 2000 [8], and has direct influence on inhibitor-interacting residues [9]. We hypothesize that reduced flexibility of the 30s and 80s loops due to molecular anchoring properties of L33F may contribute to drug resistance.

2. Materials and methods

2.1. Protein expression, purification, and crystallization

The recombinant MDR769 L33F HIV-1 protease was expressed using a T7 promoter expression vector with *Escherichia coli* BL21

Abbreviations: PR, HIV-1 protease; PI, protease inhibitor; HAART, highly active antiretroviral therapy; DRV, darunavir; MDR769, multidrug-resistant clinical isolate 769 HIV-1 protease variant; DRV/r, ritonavir pharmacokinetic boosted darunavir

* Corresponding author.
E-mail address: kovari@med.wayne.edu (L.C. Kovari).
[1] These authors contributed equally to this work.

http://dx.doi.org/10.1016/j.bbrep.2015.06.003

(DE3) as the host. MDR769 L33F is based on the previously studied multi-drug resistant variant 769, MDR769, which contains the mutations Q7K, L10I, M36V, M46L, I54V, I62V, L63P, A71V, V82T, I84V, L90M [10]. MDR769 L33F contains all mutations seen in MDR769 as well as the additional mutation L33F. Purification strategies were carried out as previously described [11,12]. Apo MDR769 L33F was crystallized using the hanging-drop vapor diffusion method. Two precipitant conditions produced crystals: (2.4 M ammonium sulfate, 0.1 M MES, pH 6.2) and (2.4 M ammonium sulfate, 0.1 M HEPES, pH 6.8). Co-crystallization methods were unable to produce high-quality crystals; therefore, apo crystals were soaked for 19 h in conditions matching the mother liquor in which they were formed, with the addition of DRV in molar excess (5 mM DRV, 5% DMSO). The crystals were cryoprotected with 30% glucose and were flash frozen in liquid nitrogen. Data were collected at the LS-CAT facility, located within Argonne National Laboratory's Advanced Photon Source.

2.2. Structure determination, refinement, and analysis

The structure of the apo L33F model was determined at a resolution of 1.50 Å. It was phased by molecular replacement (MR) using PHASER [13] with PDB entry 1TW7 as the initial search model. Refinement was performed using Phenix [14]. Subsequent structures containing a PI were phased using the apo L33F structure as a search model. The models were built in COOT [15]. After MR, ligands were added manually into the model after the protein was refined. A round of refinement was performed with PDB-REDO [16] before deposition to the protein data bank (www.pdb.org). The final models were analyzed and validated with MolProbity [17]. All images were created using PyMoL [18]. Non-covalent interactions were identified using LigPlot+ [19]. Hydrogen bonds were identified as donor–acceptor pairs with a cutoff distance of 3.2 Å; all distances were measured in PyMoL. The crystallographic data are shown in Supplementary material.

2.3. Molecular dynamics simulations

Coordinates for wild-type PR [20] (3PHV.pdb), MDR769 [10] (1TW7.pdb), and MDR769 L33F (4YOB.pdb) were used for system preparation. Crystallographic waters were retained during the initial setup. The biologically active homodimer of the protease was used for the simulations. The systems were placed in a TIP3P 5 Å water box and neutralized with magnesium chloride. MD simulations were performed as previously described [5] using NAMD [21] V. 2.9.

Trajectories of the MD simulation were analyzed using Visual Molecular Dynamics [22] (VMD) V. 1.92. Residue RMSD values were calculated using the Timeline tool in VMD by analysis of the last 10 ns of the simulation utilizing the frame corresponding to 30 ns as the reference frame.

3. Results

3.1. Structural features of the residue 33 environment

The side chain of L33F extends 2.2 Å deeper into the hydrophobic pocket compared to wild-type (WT) L33 (Fig. 1) leading to increased hydrophobic interactions between L33F and the hydrophobic pocket. The hydrophobic pocket is defined by residues I13, I15, K20, A22, T31, M/V36, L38, I64, I66, V75, V77, N83, and I85 (Fig. 1B–D). To visually identify changes in these residues, we aligned and superimposed the WT, MDR769, and MDR769 L33F structures. Although conformational and positional changes in these residues are seen between the WT and MDR769 structures (Fig. 1B and C), the L33F mutation produces further alterations in many of these residues (Fig. 1D). The most notable change is in residue I13, which rotates to avoid steric clashes with L33F. Other significant changes due to the L33F mutation are noted in residues I15, K20, A22, V36, L38, I66, and N83. These changes lead to increased hydrophobic interactions in L33F compared to the WT and MDR769 structures (Table 1).

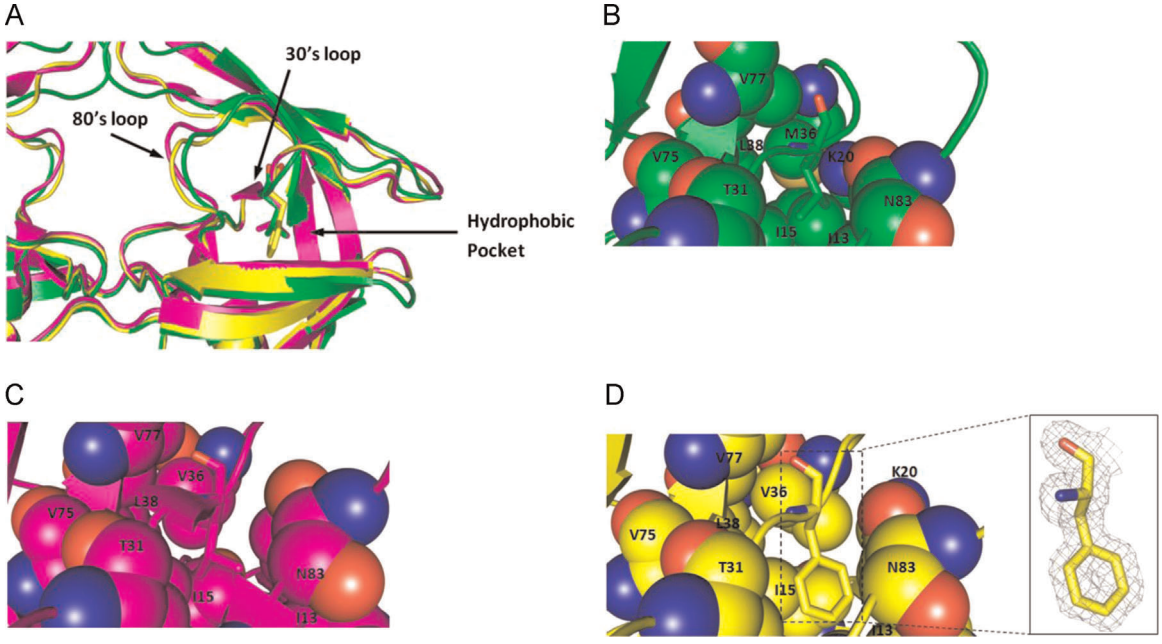

Fig. 1. Structural features of the residue 33 molecular anchor. (A) Superposition of WT protease (green), MDR769 protease (magenta), and MDR769 L33F protease (yellow) apo structures. The 30s loop, which contains residue 33, is positioned between the 80s loop and the hydrophobic pocket. In (B), (C) and (D) WT, MDR769, and MDR769 L33F are shown, respectively. Color schemes for (B–D) are as shown in (A). L33F fills the hydrophobic pocket more completely than L33. The inset in panel (D) shows the $2F_o - F_c$ map for MDR769 L33F contoured at 1σ.

Table 1
Top row: non-covalent interactions between residue 33 (L/F) and hydrophobic pocket residues. Bottom row: non-covalent interactions between DRV and active site residues. Interactions involving residue 33L/F were identified using the DimPlot script in LigPlot+; interactions between PR and DRV in the complexed structures were determined using LigPlot+. Mutations present in MDR769 reduce the number of non-covalent interactions with the hydrophobic pocket. Substitution of L33F restores the interactions between residue 33 and the hydrophobic pocket and extends them beyond what is observed in the WT structures. Interactions between DRV and the active site are reduced by mutations present in MDR769 but are further reduced due to the molecular anchoring properties of the non-polymorphic L33F mutation.

Structure name PDB code	WT apo 3PHV	WT:DRV complex 4LL3	MDR769 apo 1TW7	MDR769:DRV 3SO9	MDR769 33F apo 4YOB	MDR769 33F:DRV complex 4YOA
Residue 33L/F non-covalent interactions	30	27	24	23	32	31
DRV:non-covalent interactions	N/A	63	N/A	53	N/A	34

The MDR769 L33F structures show increased rigidity compared to the WT and MDR769 structures. Upon drug binding, L33 in the WT–DRV complex shifts 1.1 Å towards the active site and a hydrogen bond is formed between the backbone amide nitrogen of L33 and the backbone carbonyl of G78. Additionally, the side chains of residues I13, I15, M36, I66, and V75 are rotated, residues I15, K20, M36, L38, and V77 shift 0.4 Å, 1.2 Å, 2.3 Å, and 2.1 Å, respectively, into the hydrophobic pocket, and residues T31, V75, N83, and I85 shift 0.8 Å, 0.7 Å, 1.0 Å, and 0.5 Å away from the pocket. Similar changes occur in the MDR769 structures upon drug binding. However, with the L33F mutation, minimal changes in conformation or position occur in either L33F or residues of the hydrophobic pocket upon drug binding in the MDR769 L33F structure.

3.2. L33F as a molecular anchor

When the 30s loop (residues 29–35) of PR bears the L33F mutation, flexibility of both the 30s and 80s loops (residues 79–84) is decreased, likely through increased hydrophobic interactions. The 80s loop influences the S1/S1′ binding site [23], and the 30s loop lies between the 80s loop and the hydrophobic pocket (Fig. 1A). In the WT–DRV complex, drug binding causes the 30s loop residues to shift, on average, 1.5 Å towards the active site compared to the WT apo structure (Fig. 2A). In a similar fashion, the adjacent 80s loop residues also shift, on average, 2.0 Å towards the active site (Fig. 2A). Furthermore, residue 33L in the WT–DRV complex displays fewer noncovalent interactions compared to the WT apo structure (Table 1). Similar to the WT–DRV complex, the 30s and 80s loops of the MDR769–DRV complex shift 1.6 Å and 2.4 Å, respectively, towards the active site compared to the apo structure (Fig. 2B). Also, the number of noncovalent interactions is severely reduced in the MDR769 structures compared to the WT structures (Table 1). However, the 30s and 80s loops of the MDR769 L33F–DRV complex show minimal shifting upon drug binding; the only significant change is in residue P81, which shifts 0.4 Å into to the active site and puckers up when DRV is bound in the active site (Fig. 2C). In addition to the decreased flexibility of the 30s and 80s loops in the MDR769 L33F structures, the L33F mutation restores the noncovalent interactions with the hydrophobic pocket that were originally lost in the MDR769 complex. These restored interactions are also more extensively maintained than in the WT–DRV complex (Table 1). The decreased flexibility of both the 30s and 80s loops is likely due to enhanced anchoring by L33F via increased hydrophobic interactions within the hydrophobic pocket.

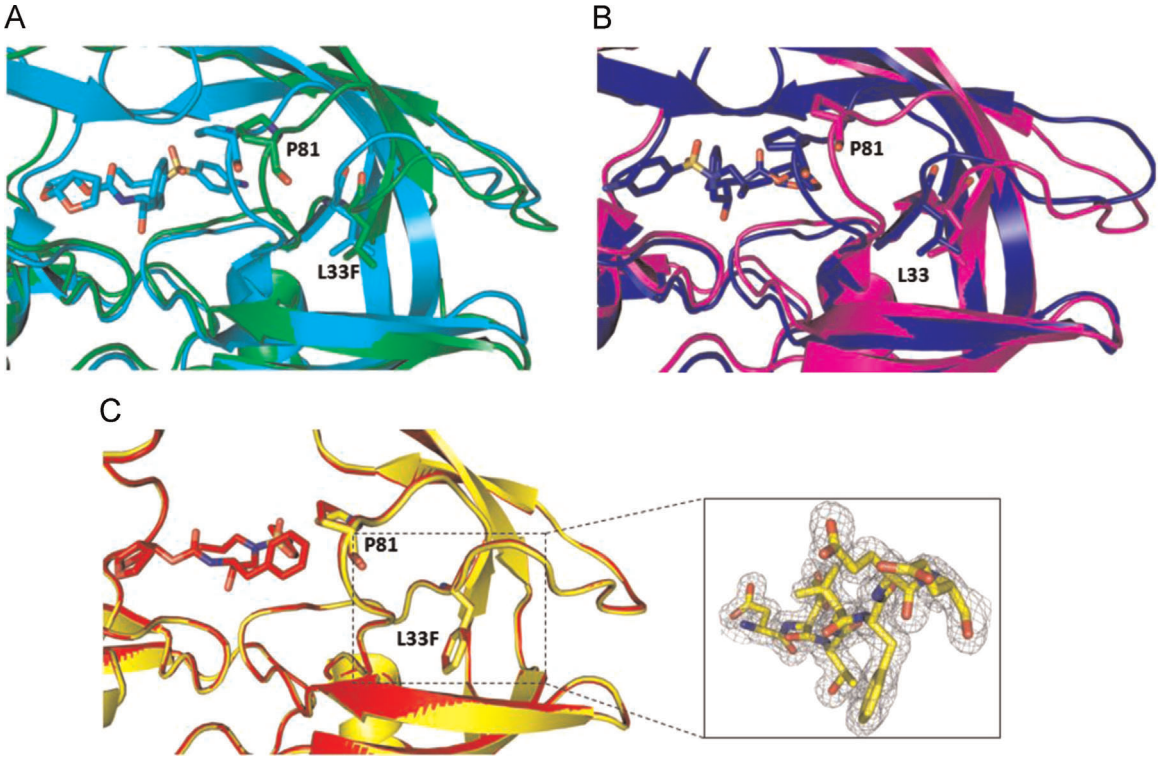

Fig. 2. L33F acts as a molecular anchor that restricts movement of the 30s and 80s loops. (A) Superposition of WT apo protease (green) and WT–DRV complex (cyan). (B) Superposition of MDR769 apo (magenta) and MDR769–DRV complex (blue). The 30s loop and 80s loop in (A) and (B) both shift with DRV bound. (C) Superposition of MDR769 33F apo (yellow) and MDR769 L33F–DRV complex (red). L33F prevents movement of the 30s and 80s loops towards the active site as in the WT and MDR769 structures. The inset in (C) shows the $2F_o - F_c$ map for the 30s loop residues (D29–E35) contoured at 1σ.

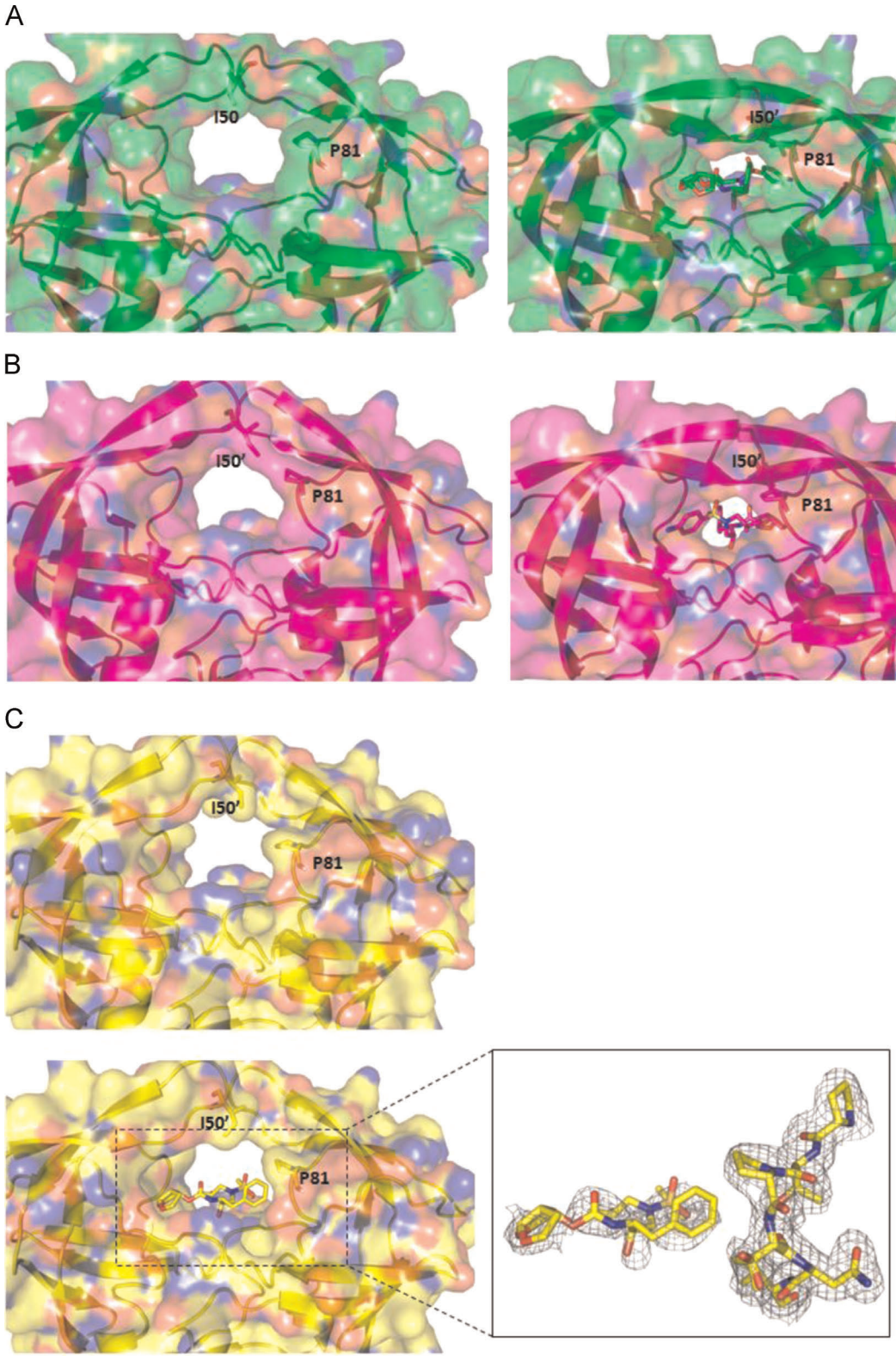

Fig. 3. Reduced flap interactions due to L33F anchoring. (A) WT apo protease and WT protease complexed with DRV. The apo WT shows a 7.5 Å gap between P81 of the 80s loop and I50 of the flap producing an active site in the open conformation. When complexed with DRV, the flaps and active site close. (B) MDR769 apo protease and MDR769–DRV complex. Despite interactions between the 80s loop and flaps in the MDR769 protease, the flaps and active site display an open conformation. With DRV in the active site, the flexibility of MDR769 protease produces a closed active site. (C) MDR769 L33F apo PR and MDR769 L33F complexed with DRV bound resembles the WT apo structure in (A) with a large gap between residues I50′ and P81. The gap between I50′ and P81 is maintained between the apo and complexed structures (5.8 Å and 5.9 Å, respectively) and is too large for interactions to occur. The active site and S1/S1′ subsite remain open. The inset in (C) shows the $2F_o - F_c$ map for DRV and the 80s loop in the L33F structure contoured at 0.5σ in order that the density around DRV is shown.

To further assess the hypothesis of L33F acting as a molecular anchor, 40 ns MD simulations were performed. Differences in protein flexibility due to molecular anchoring of L33F should be more pronounced in apo PR compared to PI-complexed forms. Therefore the RMSD of the 30s and 80s loops for both chains of apo WT, MDR769, and MDR769 L33F were analyzed over the last 10 ns. For WT PR, the average RMSD values of the 30s and 80s loops were 1.53 Å and 1.65 Å, respectively. The 30s loop of the MDR769 structure showed reduced flexibility compared to the WT structure with an RMSD of 1.34 Å whereas the 80s loop of the MDR769 showed similar flexibility compared to the WT (1.66 Å). Flexibility of the 30s and 80s loops in MDR769 L33F were further reduced compared to both WT and MDR769 structures with the 30s loop displaying an RMSD of 1.27 Å and the 80s loop displaying an RMSD of 1.55 Å (Fig. S1).

3.3. Reduced flap interactions and altered drug conformation

Previous work documented interactions between the 80s loop and the flap tips [24], their importance in substrate recognition and binding [25], and their influence on forming the S1/S1′ subsite [23]. Thus, effects of the L33F mutation on the 80s loop and flap tips are possibly implicated in resistance development.

In the WT protease, the flexibility of the 80s loop and flaps produces favorable interactions allowing for proper formation of the S1/S1′ subsite. In the WT apo structure, a large 7.5 Å gap between the P81 of the 80s loop and I50 of the flap tips exists, preventing any interactions between the two (Fig. 3A). However, with DRV bound in the active site, the flaps close and the 80s loop shifts (2.0 Å) towards the active site which brings P81 within 3.7 Å of G49′ and T80 within 3.9 Å of I50′ (Fig. 3A). These distances allow for favorable interactions between the flap and the 80s loop resulting in a closed active site, and more specifically, a properly formed S1/S1′ subsite (Fig. 3A). As a result, DRV makes extensive noncovalent interactions with the residues lining the active site as indicated in Table 1.

Similar to the WT protease, the MDR769 protease displays considerable flexibility in the 30s and 80s loops (Fig. 3B). The gap between residues P81 and I50′ in the MDR apo structure is not large compared to the WT (3.6 Å compared to 7.5 Å). The flaps are in a “wide-open” conformation as reported previously [10], which leaves the active site open. In the MDR769–DRV complex, the flexibility of the 30s and 80s loops (Fig. 2B) allows the active site to close (Fig. 3B). Even though the active site is closed, the number of noncovalent interactions between DRV and the active site is decreased, suggesting a slightly distorted active site (Table 1).

In the MDR769 L33F apo structure, the gap between the 80s loop and the flaps resembles the WT apo structure, producing an open active site and an open S1/S1′ subsite. The apo structure contains a 5.8 Å gap between P81 and I50′; this gap is smaller than the WT but still too large for any significant interactions to occur. In the L33F–DRV complex, P81 shifts 0.4 Å into the active site, but I50′ also shifts and rotates leaving a 5.9 Å gap which resembles the WT apo structure (Fig. 3C). The 5.9 Å gap between P81 and I50′ leaves an open S1/S1′ subsite and also results in an open active site. The result is a severely reduced number of interactions between DRV and the active site compared to both the WT and MDR769 structures (Table 1).

Additionally, in the L33F–DRV complex, the side chains of P2, P1, and P1′ of DRV are rotated to compensate for the open S1/S1′ subsite (Fig. 3C) which alters the hydrogen-bonding network compared to the WT–DRV complex. Previous reports have indicated a conserved hydrogen bonding network between DRV and backbone and side-chain atoms of residues D25, G27, D29, D30, D25′, and D30′ [26]. In the WT–DRV complex, the P2 *bis*-THF moiety, hydroxyl, and P2′ amine of DRV are responsible for formation of five hydrogen bonds with residues D25, D29, D30, D25′, and D30′ (data not shown). However, the L33F–DRV complex contains an expanded active site and S1/S1′ subsite which alters the conformation of P2, P1, P1′, and P2′ of DRV. As a result, the P2 *bis*-THF moiety, hydroxyl, and P2′ amine of DRV form only three hydrogen bonds with residues D25N, D30, and D29′. Additionally, the number of contacts decreased between the P1 group of DRV and the residues of the S1/S1′ subsite (Table 1).

4. Discussion

The L33F mutation is selected in patients receiving a DRV/r regimen [3], and is associated with reduced response to DRV/r treatment [4,7] as it has direct influence on the inhibitor-interacting residues [9]. This report describes the effects of L33F on the structure of HIV protease as well as the effect it has on inhibitor recognition.

Superposition of MDR769 L33F with WT and MDR769 HIV-1 PR with and without DRV in the active site reveals altered conformation of the 30s and 80s loops. The larger side chain of L33F embeds further into the hydrophobic pocket than L33, the latter of which is present in both WT and MDR769 structures (Fig. 1). As a result, noncovalent interactions are increased in this region compared to the WT, causing the L33F to act as a molecular anchor. MD simulations showed a clear reduction in flexibility of both the 30s and 80s loops for MDR769 L33F compared to both WT and MDR769. The results of these simulations support the hypothesis that L33F may play a role as a molecular anchor within HIV-1 protease.

Enhanced molecular anchoring by the L33F mutation reduces the flexibility of the 30s and 80s loops, thereby inhibiting proper formation of the S1/S1′ subsite and keeping the active site in an open conformation in the MDR769 L33F–DRV complex (Figs. 2 and 3). Conversely, in the WT and MDR769 complex structures, DRV binding causes a shift in the 30s and 80s loops leading to formation of the S1/S1′ subsite and closing of the active site (Figs. 2 and 3).

The structure of the L33F DRV complex reported here shows the protease flaps in an open conformation. To date, all deposited structures of HIV PR L33F complexes have been solved in three different space groups: $P2_12_12_1$, $P6_1$, and $P4_12_12$. The majority of these HIV PR L33F DRV complexes have been solved with the flaps in a closed conformation. Other research groups such as the Schiffer group [27] and the Konvalinka group [28] have previously reported L33F DRV complexes with the flaps in a closed conformation by solving the structures in $P2_12_12_1$ (PDB ID:4QY1) and $P6_1$ (PDB ID:3GGU), respectively. In contrast, the Weber group [29] and this report describe the L33F DRV complex as a structure with open protease flaps when the structures were solved in $P4_12_12$. The Weber group [29] (PDB ID:4NPT) also utilized the inactivating mutation D25N to facilitate HIV PR expression, purification, and crystallization.

With specific regard to the L33F mutation, the Schiffer group (closed protease flaps) reports L33F may play a role in active site expansion [27]. The Konvalinka group (closed protease flaps) suggests that L33F is possibly implicated in structural changes in the flap and flap hinge regions of PR. Despite structural and symmetry differences between the aforementioned and this report, our results regarding L33F as a molecular anchor are consistent with the previous reports by the the Schiffer and Konvalinka groups. A key finding of our report is the influence of the L33F mutation on the open active site and on the S1/S1′ subsites through anchoring of the 30s and 80s loops independent of space group.

In conclusion, for the first time we here report the molecular mechanisms by which the nonpolymorphic PR mutation L33F contributes to DRV resistance. The L33F mutation may contribute to resistance via two mechanisms: one, by restoring noncovalent interactions lost due to other primary mutations, and two, by further reducing interactions between DRV and active site residues. These findings may contribute to our overall understanding of drug resistance as well as future drug design strategies. We propose that modifications to the P1/P1′ groups of existing PIs to fill the open S1/S1′ subsite might result in a greater response by patients who harbor the L33F mutation in HIV-PR.

Acknowledgments

We thank the National Institutes of Health, USA (grant no. NIH: AI065294) for funding to LCK. Use of the Advanced Photon Source, an Office of Science User Facility operated by the U.S. Department of Energy (DOE) Office of Science by Argonne National Laboratory, was supported by the DOE, USA under Contract no. DE-AC02-06CH1 1357.

Appendix A. Supplementary material

Supplementary data associated with this article can be found in the online version at http://dx.doi.org/10.1016/j.bbrep.2015.06.003.

References

[1] M.W. Tang, R.W. Shafer, HIV-1 antiretroviral resistance: scientific principles and clinical applications, Drugs 72 (2012) e1–25.
[2] V. Spagnuolo, N. Gianotti, E. Seminari, L. Galli, G. Fusetti, S. Salpietro, A. Lazzarin, A. Castagna, Changes in darunavir/r resistance score after previous failure to tipranavir/r in HIV-1-infected multidrug-resistant patients, J. Acquir. Immune Defic. Syndr. 50 (2009) 192–195.
[3] S. Lambert-Niclot, P. Flandre, A. Canestri, G. Peytavin, C. Blanc, R. Agher, C. Soulie, M. Wirden, C. Katlama, V. Calvez, A.G. Marcelin, Factors associated with the selection of mutations conferring resistance to protease inhibitors (PIs) in PI-experienced patients displaying treatment failure on darunavir, Antimicrob. Agents Chemother. 52 (2008) 491–496.
[4] S.Y. Rhee, M.J. Gonzales, R. Kantor, B.J. Betts, J. Ravela, R.W. Shafer, Human immunodeficiency virus reverse transcriptase and protease sequence database, Nucleic Acids Res. 31 (2003) 298–303.
[5] P.D. Chordia, G. Tamaria, Bradley Keusch, Benjamin D. Kuiper, Kyla Ross, Iulia A. Kovari, Rodger MacArthur, Hossein Salimnia, Ladislau C., Kovari, The role of mutations at codons 32, 47, 54, and 90 in HIV-1 protease flap dynami, Discoveries 2 (2014) e27.
[6] M. Maguire, D. Shortino, A. Klein, W. Harris, V. Manohitharajah, M. Tisdale, R. Elston, J. Yeo, S. Randall, F. Xu, H. Parker, J. May, W. Snowden, Emergence of resistance to protease inhibitor amprenavir in human immunodeficiency virus type 1-infected patients: selection of four alternative viral protease genotypes and influence of viral susceptibility to coadministered reverse transcriptase nucleoside inhibitors, Antimicrob. Agents Chemother. 46 (2002) 731–738.
[7] A.M. Wensing, V. Calvez, H.F. Gunthard, V.A. Johnson, R. Paredes, D. Pillay, R. W. Shafer, D.D. Richman, Update of the drug resistance mutations in HIV-1, Top. Antivir. Med. 22 (2014) 642–650.
[8] V. Varghese, Y. Mitsuya, W.J. Fessel, T.F. Liu, G.L. Melikian, D.A. Katzenstein, C. A. Schiffer, S.P. Holmes, R.W. Shafer, Prototypical recombinant multi-protease inhibitor resistant infectious molecular clones of human immunodeficiency virus type-1, Antimicrob. Agents Chemother. 57 (2013) 4290–4299.
[9] J. Agniswamy, C.H. Shen, A. Aniana, J.M. Sayer, J.M. Louis, I.T. Weber, HIV-1 protease with 20 mutations exhibits extreme resistance to clinical inhibitors through coordinated structural rearrangements, Biochemistry 51 (2012) 2819–2828.
[10] P. Martin, J.F. Vickrey, G. Proteasa, Y.L. Jimenez, Z. Wawrzak, M.A. Winters, T. C. Merigan, L.C. Kovari, "Wide-open" 1.3 A structure of a multidrug-resistant HIV-1 protease as a drug target, Structure 13 (2005) 1887–1895.
[11] Y. Wang, T.G. Dewdney, Z. Liu, S.J. Reiter, J.S. Brunzelle, I.A. Kovari, L.C. Kovari, Higher desolvation energy reduces molecular recognition in multi-drug resistant HIV-1 protease, Biology, 1, Basel (2012), p. 81–93.
[12] J.F. Vickrey, B.C. Logsdon, G. Proteasa, S. Palmer, M.A. Winters, T.C. Merigan, L. C. Kovari, HIV-1 protease variants from 100-fold drug resistant clinical isolates: expression, purification, and crystallization, Protein Expr. Purif. 28 (2003) 165–172.
[13] A.J. McCoy, R.W. Grosse-Kunstleve, P.D. Adams, M.D. Winn, L.C. Storoni, R. J. Read, Phaser crystallographic software, J. Appl. Crystallogr. 40 (2007) 658–674.
[14] P.D. Adams, P.V. Afonine, G. Bunkoczi, V.B. Chen, I.W. Davis, N. Echols, J. J. Headd, L.W. Hung, G.J. Kapral, R.W. Grosse-Kunstleve, A.J. McCoy, N. W. Moriarty, R. Oeffner, R.J. Read, D.C. Richardson, J.S. Richardson, T. C. Terwilliger, P.H. Zwart, PHENIX: a comprehensive python-based system for macromolecular structure solution, Acta Crystallogr. D: Biol. Crystallogr. 66 (2010) 213–221.
[15] P. Emsley, K. Cowtan, Coot: model-building tools for molecular graphics, Acta Crystallogr. D: Biol. Crystallogr. 60 (2004) 2126–2132.
[16] R.P. Joosten, J. Salzemann, V. Bloch, H. Stockinger, A.C. Berglund, C. Blanchet, E. Bongcam-Rudloff, C. Combet, A.L. Da Costa, G. Deleage, M. Diarena, R. Fabbretti, G. Fettahi, V. Flegel, A. Gisel, V. Kasam, T. Kervinen, E. Korpelainen, K. Mattila, M. Pagni, M. Reichstadt, V. Breton, I.J. Tickle, G. Vriend, PDB_REDO: automated re-refinement of X-ray structure models in the PDB, J. Appl. Crystallogr. 42 (2009) 376–384.
[17] V.B. Chen, W.B. Arendall 3rd, J.J. Headd, Keedy, R.M. Immormino, G.J. Kapral, L. W. Murray, J.S. Richardson, D.C. Richardson, MolProbity: all-atom structure validation for macromolecular crystallography, Acta Crystallogr. D: Biol. Crystallogr. 66 (2010) 12–21.
[18] L.L.C. Schrodinger, The PyMOL Molecular Graphics System Version 1.3r1, 2010.
[19] R.A. Laskowski, M.B. Swindells, LigPlot+: multiple ligand-protein interaction diagrams for drug discovery, J. Chem. Inf. Model. 51 (2011) 2778–2786.
[20] R. Lapatto, T. Blundell, A. Hemmings, J. Overington, A. Wilderspin, S. Wood, J. R. Merson, P.J. Whittle, D.E. Danley, K.F. Geoghegan, et al., X-ray analysis of HIV-1 proteinase at 2.7 A resolution confirms structural homology among retroviral enzymes, Nature 342 (1989) 299–302.
[21] J.C. Phillips, R. Braun, W. Wang, J. Gumbart, E. Tajkhorshid, E. Villa, C. Chipot, R. D. Skeel, L. Kale, K. Schulten, Scalable molecular dynamics with NAMD, J. Comput. Chem. 26 (2005) 1781–1802.
[22] W. Humphrey, A. Dalke, K. Schulten, VMD: visual molecular dynamics, J. Mol. Graph. 14 (1996) 33–38 27–38.
[23] R.S. Yedidi, G. Proteasa, J.L. Martinez, J.F. Vickrey, P.D. Martin, Z. Wawrzak, Z. Liu, I.A. Kovari, L.C. Kovari, Contribution of the 80s loop of HIV-1 protease to the multidrug-resistance mechanism: crystallographic study of MDR769 HIV-1 protease variants, Acta Crystallogr. D: Biol. Crystallogr. 67 (2011) 524–532.
[24] F. Liu, A.Y. Kovalevsky, Y. Tie, A.K. Ghosh, R.W. Harrison, I.T. Weber, Effect of flap mutations on structure of HIV-1 protease and inhibition by saquinavir and darunavir, J. Mol. Biol. 381 (2008) 102–115.
[25] Z. Liu, Y. Wang, R.S. Yedidi, T.G. Dewdney, S.J. Reiter, J.S. Brunzelle, I.A. Kovari, L.C. Kovari, Conserved hydrogen bonds and water molecules in MDR HIV-1 protease substrate complexes, Biochem. Biophys. Res. Commun. 430 (2013) 1022–1027.
[26] R.S. Yedidi, H. Garimella, M. Aoki, H. Aoki-Ogata, D.V. Desai, S.B. Chang, D. A. Davis, W.S. Fyvie, J.D. Kaufman, D.W. Smith, D. Das, P.T. Wingfield, K. Maeda, A.K. Ghosh, H. Mitsuya, A conserved hydrogen-bonding network of P2 bis-tetrahydrofuran-containing HIV-1 protease inhibitors (PIs) with a protease active-site amino acid backbone aids in their activity against PI-resistant HIV, Antimicrob. Agents Chemother. 58 (2014) 3679–3688.
[27] D.A. Ragland, E.A. Nalivaika, M.N. Nalam, K.L. Prachanronarong, H. Cao, R. M. Bandaranayake, Y. Cai, N. Kurt-Yilmaz, C.A. Schiffer, Drug resistance conferred by mutations outside the active site through alterations in the dynamic and structural ensemble of HIV-1 protease, J. Am. Chem. Soc. 136 (2014) 11956–11963.
[28] K.G. Saskova, M. Kozisek, P. Rezacova, J. Brynda, T. Yashina, R.M. Kagan, J. Konvalinka, Molecular characterization of clinical isolates of human immunodeficiency virus resistant to the protease inhibitor darunavir, J. Virol. 83 (2009) 8810–8818.
[29] Y. Zhang, Y.C. Chang, J.M. Louis, Y.F. Wang, R.W. Harrison, I.T. Weber, Chem. Biol. 9 (2014) 1351–1358.